RPE Radiation Physics & Engineering
An International Peer-Reviewed Journal
Published by K.N. Toosi University of Technology
http://rpe.kntu.ac.ir
Research Article

Radiation Physics and Engineering 2020; 1(1):19–27
https://doi.org/10.22034/RPE.2020.57885

Three-dimensional solution of the forward and adjoint neutron diffusion equation using the generalized least squares finite element method

Farahnaz Saadatian-Derakhshandeh*
MASNA Engineering Company, P.O. Box 1439951113, Tehran, Iran.

HIGHLIGHTS

- Multi-group static 3-D neutron diffusion equation is solved using the finite element method.
- Generalized least squares FEM, through a variational approach is applied for solving the NDE.
- GELES code is developed based on the tetrahedral elements for an arbitrary shaped system.
- To validate the approach, output of GELES were compared against the DONJON computer code.
- Acceptable accuracy for the neutron multiplication factor and the power distribution was achieved.

ABSTRACT

Numerical solution of the multi-group static forward and adjoint neutron diffusion equation (NDE) using the Finite Elements Method (FEM) is investigated in detail. A finite element approach based on the generalized least squares method is applied for the spatial discretization of the NDE in 3D-XYZ geometry. A computer code called GELES was also developed based on the described methodology covering linear or quadratic tetrahedral elements generated via the mesh generator for an arbitrary shaped system. A number of test cases are also studied to validate the proposed approach. Moreover, to assess the output dependency to the number of elements, a sensitivity analysis is carried out at the end.

KEYWORDS
Neutron Diffusion Equation
Adjoint Flux
Generalized Least Squares
Finite Element Method

HISTORY
Received: 29 September 2017
Revised: 10 November 2017
Accepted: 5 January 2018
Published: January 2020

1 Introduction

Various techniques *e.g.* finite difference, finite element, boundary element or finite volume methods might be employed for the numerical solution of differential equations arising in engineering problems. However, the Finite Elements Method (FEM) has proved its superiority for a wide range of problems thanks to its firm theoretical basis as well as fair applicability in industrial scale engineering challenges.

The basic idea in the finite element method is to find the solution to a complicated problem through replacing it by a simpler one and to obtain an admissible approximate solution rather than the exact. The first application of FEM to the theory of neutron diffusion dates back to 1970s (Kang and Hansen, 1973). The development in the application of FEM to the Neutron diffusion equation (NDE) has been described in the excellent treatise of (Lewis, 1981). Recently, several other applications of FEMs including Thomas-Raviart-Schneider, hybrid, h-adaptivity, response matrix, etc. to solve NDE has been introduced (Cavdar and Ozgener, 2004; Hébert, 2008; Wang et al., 2009).

The current study focuses on the application of the generalized least squares FEM, through a variational approach for solving the multi-group forward/adjoint NDE for reactor cores with 3D Cartesian geometry. As a considerable privilege, internal incorporation of boundary conditions makes the approach much easier than other methods. The approach is utilized for the development of a computational code, called GELES, able to solve multigroup forward/adjoint NDE for systems with arbitrary geometry in 3D space. Linear and quadratic tetrahedral finite elements generated by a mesh generator are supported by the GELES. Indeed, a key advantage of tetrahedral elements is their superiority in fair filling of objects with curved boundaries or arbitrary oriented interfaces.

An outline of the remainder of this contribution is as follows: In section 2, we briefly introduce the application of generalized least squares method for a variational formulation of NDE. Section 3 is devoted to the discretization scheme used for maximizing the variational principle ob-

*Corresponding author: Saadatian83@yahoo.com

tained through the generalized least squares method. A number of benchmark problems solved through the proposed methodology are presented in section 4. Outcome sensitivity to the degrees of freedom is also investigated in this section. A discussion on the outcome of the code for benchmark problems in given in section 5, and we will finally sum up the paper with a conclusion in section 6.

2 Generalized Least Squares Finite Element Method

The generalized least squares method is a variational approach able to approximate the solution of NDE via minimizing the sum of the residual squares of the result. The method was shown to provide a simple approach for establishing variational principles for the finite elements treatment of diffusion theory (Ackroyd, 1986a). In this method, a residual is defined as the difference between the actual values of the neutron flux and current, and the values predicted. Consider $\Phi \equiv \{\phi, \mathbf{J}\}$ as the approach vector and $\Phi_0 \equiv \{\phi_0, \mathbf{J}_0\}$ as the actual results vector, the squares of the errors vector would be:

$$\mathcal{H}(\phi, \mathbf{J}) \equiv (\Phi - \Phi_0)^2 = \{(\phi - \phi_0)^2, (\mathbf{J} - \mathbf{J}_0)^2\} \quad (1)$$

and, other vectors are defined as follows:

$$\begin{aligned} \Phi' &\equiv \{\phi, 0\} \\ \Phi'_0 &\equiv \{\phi_0, 0\} \\ \tilde{\Phi} &\equiv \{\phi, \mathbf{J}_0\} \end{aligned} \quad (2)$$

where

$$\tilde{\Phi} - \Phi_0 = \Phi' - \Phi'_0. \quad (3)$$

Also, the square of the error value can be defined as

$$(\Phi' - \Phi'_0)^2 = (\Phi'_0)^2 + (\Phi')^2 - 2\Phi'_0.\Phi'. \quad (4)$$

McConnell (McConnell, 1951) followed by Ackroyd (Ackroyd, 1986b) have far previously explained the relationship between classical variational principles and the scalar product in the Hilbert space. Scalar product of two arbitrary vectors φ_1 and φ_2 (of the kind of those introduced by Eq. (2)) for a multi-region body with volume V in Hilbert space is defined as

$$\begin{aligned} \varphi_1.\varphi_2 = &\int_V \{(R_1 \mathcal{A} R_1) + (R_2 \mathcal{B} R_2)\} \mathrm{d}V \\ &+ \int_{\cup(S_i \cap S_j)} \{\mathcal{W}[\phi_1]_{r-0}^{r+0}[\phi_2]_{r-0}^{r+0} \\ &+ \mathcal{W}'[\mathbf{J}_1]_{r-0}^{r+0}[\mathbf{J}_2]_{r-0}^{r+0}\} \mathrm{d}S \\ &+ \int_{S_{ext}} \mathcal{W}[\phi_1 - \alpha^2 \mathbf{n}.\mathbf{J}_1][\phi_2 - \alpha^2 \mathbf{n}.\mathbf{J}_2] \mathrm{d}S \end{aligned} \quad (5)$$

Where, $\mathcal{A}$ and $\mathcal{B}$ are two self-adjoint and positive definite operators, R_1 and R_2 are the residuals which provide a measure of errors made by the function ϕ as approximate solution of the NDE, $\mathcal{W}$ is an arbitrary weight coefficient, $S_i \cap S_j$ is the interface of regions i and j, and S_{ext} denotes the external boundary with the normal vector $\mathbf{n}$. S_{ext} can be either a zero flux, reflective or extrapolated boundary depending on the value of α. In Eq. (5) the first integral is taken over the residual values (R_1 and R_2) obtained across the volume due to approximation used for the NDE, the second integral is the error value obtained from the neutron flux and current discontinuities at interfaces that are admissible. Finally, the third integral is related to the mismatch for a perfect reflector at external boundaries. The notation used for discontinuities is shown in Fig. 1 (Ackroyd, 1986b).

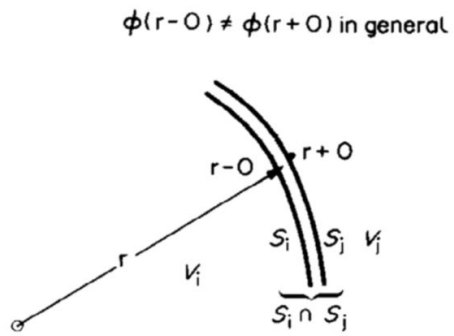

Figure 1: Discontinuities at interfaces of the regions (Ackroyd, 1986b).

Therefore, as an example, for a two region geometry shown in Fig. 2 each of the terms in Eq. (4) can be obtained as a scalar product of two vectors according to Eq. (5) as

$$\begin{aligned} (\Phi'_0)^2 = &\int_V [(\Sigma_a \phi_0 \mathcal{A} \Sigma_a \phi_0) + (D\nabla\phi_0 \mathcal{B} D \nabla\phi_0)] \mathrm{d}V \\ &+ \int_{S_2} \mathcal{W}\phi_0^2 \mathrm{d}S \end{aligned} \quad (6)$$

$$\begin{aligned} (\Phi')^2 = &\int_V [(\Sigma_a \phi \mathcal{A} \Sigma_a \phi) + (D\nabla\phi \mathcal{B} D \nabla\phi)] \mathrm{d}V \\ &+ \int_{S_1} [\phi \mathbf{n}.\mathbf{J}]_{r-0}^{r+0} + \int_{S_2} \mathcal{W}\phi^2 \mathrm{d}S \end{aligned} \quad (7)$$

$$\begin{aligned} \Phi'_0.\Phi' = &\int_V [(\Sigma_a \phi_0 \mathcal{A} \Sigma_a \phi) + (D\nabla\phi_0 \mathcal{B} D \nabla\phi)] \mathrm{d}V \\ &+ \int_{S_1} [\phi \mathbf{n}.\mathbf{J}_0]_{r-0}^{r+0} + \int_{S_2} \mathcal{W}\phi\phi_0 \mathrm{d}S \end{aligned} \quad (8)$$

where ∇ is the Nabla operator, and Σ_a and D are Macroscopic absorption XS and Diffusion constant, respectively. In Eqs. (6-8), it was assumed that entry current value on the outer boundary of the system is zero and also, neutron flux values on the inner boundaries are continuous.

By use of the neutron balance equation in the presence of a neutron source ($\mathcal{S}$), absorption rate is as follows:

$$\Sigma_a(r)\phi_0(r) = \mathcal{S}(r) - \nabla.\mathbf{J}_0 \quad (9)$$

According to the Fick's law, Eq. (8) can be written as

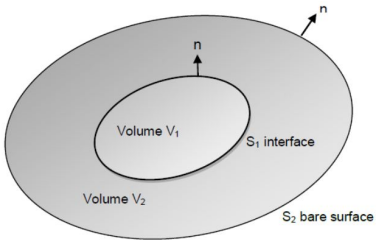

Figure 2: A sample system with two regions.

$$\Phi_0'.\Phi' = \int_V [(\mathcal{S}\mathcal{A}\Sigma_a\phi) + (\nabla.\mathbf{J}_0\mathcal{A}\Sigma_a\phi) - (\mathbf{J}_0\mathcal{B}D\nabla\phi)]\mathrm{d}V + \int_{S_1} [\phi\mathbf{n}.\mathbf{J}_0]_{r-0}^{r+0}\mathrm{d}S + \int_{S_2} \mathcal{W}\phi\phi_0\mathrm{d}S \tag{10}$$

It is supposed that $\mathcal{A}\Sigma_a = \mathcal{B}D = 1$ and by the properties of operator ∇ plus the divergence theorem we have

$$\nabla.(\mathbf{J}_0\phi) = (\nabla.\mathbf{J}_0)\phi + \mathbf{J}_0.\nabla\phi \tag{11}$$

$$\int_V \nabla.(\mathbf{J}_0\phi)\mathrm{d}V = \oint_{\mathcal{S}} \phi(\mathbf{J}_0.\mathbf{n})\mathrm{d}S. \tag{12}$$

Hence, Eq. (10) becomes

$$\Phi_0'.\Phi' = \int_V \mathcal{S}\phi\mathrm{d}V + \int_{S_1} [\phi(\mathbf{J_0}.\mathbf{n})]_{r-0}^{r+0}\mathrm{d}S + \int_{S_2} \phi(\mathcal{W}\phi_0 - \mathbf{J_0}.\mathbf{n})\mathrm{d}S. \tag{13}$$

For the bare boundary condition there would be

$$\phi(r_s) - \alpha^2\mathbf{n}.\mathbf{J}(r_s) = 0, \quad \alpha^2 = 2. \tag{14}$$

If $\mathcal{W} = \dfrac{1}{\alpha^2}$ and flux values on the inner boundaries are assumed continuous, Eq. (13) is turned to

$$\Phi_0'.\Phi' = \int_V \mathcal{S}\phi\mathrm{d}V. \tag{15}$$

Using a similar procedure for Eq. (7) we may have

$$(\Phi')^2 = \int_V [(\phi\Sigma_a\phi) + (\nabla\phi.D\nabla\phi)]\mathrm{d}V + \frac{1}{\alpha^2}\int_{S_2} \phi^2\mathrm{d}S. \tag{16}$$

Now, a variational principle, $K'[\phi]$ can be defined from the combination of Eqs. (15) and (16) as

$$\begin{aligned} K'[\varphi] \equiv& 2\Phi_0'.\Phi' - (\Phi')^2 \\ =& 2\int_V (\mathcal{S}\phi)\mathrm{d}V - \int_V [(\phi\Sigma_a\phi) + (\nabla\phi.D\nabla\phi)]\mathrm{d}V \\ &- \frac{1}{\alpha^2}\int_{S_2} \phi^2\mathrm{d}S. \end{aligned} \tag{17}$$

Hence, Eq. (4) can now be rewritten as

$$(\Phi' - \Phi_0')^2 = (\Phi_0')^2 - K'[\phi]. \tag{18}$$

Non-zero *lhs* of Eq. (18) reveals that

$$K'[\varphi] \leq (\Phi_0')^2 \tag{19}$$

As a consequence, maximizing $K'[\varphi]$ principle defined by Eq. (17) minimizes the error. Now, $K'[\varphi]$ value is a maximum variational principle to solve the NDE by using of the generalized least squares method. As seen it is not required to apply the boundary conditions since these conditions have been exerted to extract the principle, previously. Finally, the variational principle is maximized using the FEM approximation.

3 Discretization of the neutron diffusion equation

3.1 Forward neutron diffusion equation

In the absence of external neutron source, the multi-group NDE is written as (Lamarsh, 1975):

$$-D_g\nabla^2\phi_g(r) + \Sigma_{r,g}\phi_g(r) = \frac{\chi_g}{k_{eff}}\sum_{g'=1}^{G} \nu\Sigma_{f,g'}\phi_{g'}(r) + \sum_{g'\neq g} \Sigma_{g'\to g}\phi_{g'}(r), \quad g = 1, 2, ..., G \tag{20}$$

where $\phi_g(r)$ is the neutron flux in energy group g. There are D_g diffusion constant, $\Sigma_{r,g}$ macroscopic removal XS, χ_g neutron spectrum and $\Sigma_{f,g'}$ macroscopic fission XS in energy group g'. ν denotes the fission neutron yield. Also, $\Sigma_{g'\to g}$ is macroscopic scattering XS from energy group g' to g and k_{eff} is neutron multiplication factor. Eq. (20) is a linear partial differential equation which may be solved by different numerical methods. All of these methods transform the differential equation into a system of algebraic equations. Here, a FEM based on the generalized least squares method is exploited to discretize the aforementioned NDE. To start the discretization, the whole system is divided into the tetrahedral elements as shown in Fig. 3. The simplest solid element is four node tetrahedral. This is also called the linear tetrahedral since its shape functions are linear polynomials. Whereas, its quadratic approximation has ten node that is tetrahedral element including mid-side nodes. Geometry discretization could be carried out using various mesh generators such as Gambit, ABAQUS, ANSYS, and TRELIS etc.

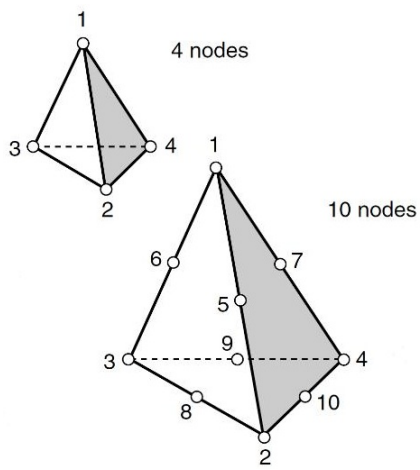

Figure 3: The linear and quadratic tetrahedral elements.

Linear or quadratic approximation of the neutron flux inside each finite element could be considered as:

$$\phi^{(e)}(x,y,z) \cong \sum_{n=1}^{P} N_n^{(e)}(x,y,z)\psi_n^{(e)} = \mathbf{N}^{(e)\mathrm{T}}.\Psi^{(e)}; \quad P = \begin{cases} 4 & \textit{linear tetrahedron} \\ 10 & \textit{quadratic tetrahedron} \end{cases} \tag{21}$$

where $N_n^{(e)}$ is the shape function associated with node n of the element e, and $\psi_n^{(e)}$ denotes the flux value over that node. Also, $\mathbf{N}^{(e)}$ and $\Psi^{(e)}$ are the corresponding vectors encapsulating $N_n^{(e)}$ and $\psi_n^{(e)}$, respectively.

For the linear approximation we may have (Zienkiewicz and Taylor, 2005):

$$N_n^{(e)}(x,y,z) = L_n^{(e)}(x,y,z) = \frac{a_n + b_n x + c_n y + d_n z}{6V_n^{(e)}}; \; n = 1,...,4 \tag{22}$$

Where $L_n^{(e)}$ is a local coordinate with the following coefficients:

$$a_1 = \begin{vmatrix} x_2 & y_2 & z_2 \\ x_3 & y_3 & z_3 \\ x_4 & y_4 & z_4 \end{vmatrix}; \quad b_1 = -\begin{vmatrix} 1 & y_2 & z_2 \\ 1 & y_3 & z_3 \\ 1 & y_4 & z_4 \end{vmatrix}; \quad c_1 = -\begin{vmatrix} x_2 & 1 & z_2 \\ x_3 & 1 & z_3 \\ x_4 & 1 & z_4 \end{vmatrix}; \quad d_1 = -\begin{vmatrix} x_2 & y_2 & 1 \\ x_3 & y_3 & 1 \\ x_4 & y_4 & 1 \end{vmatrix}. \tag{23}$$

Other constants ($n = 2, 3, 4$) are defined through clockwise cyclic interchange. Also, the element volume in Eq. (22) is calculated via:

$$6V^{(e)} = \begin{vmatrix} 1 & x_1 & y_1 & z_1 \\ 1 & x_2 & y_2 & z_2 \\ 1 & x_3 & y_3 & z_3 \\ 1 & x_4 & y_4 & z_4 \end{vmatrix}. \tag{24}$$

For the quadratic approximation, shape functions are defined as:

$$N_n^{(e)}(x,y,z) = \begin{cases} (2L_n^{(e)} - 1)L_n^{(e)} & n = 1,...,4 \quad (\textit{corner nodes}) \\ 4L_i^{(e)}L_j^{(e)} & \mathbf{r}_n = (\mathbf{r}_i + \mathbf{r}_j)/2 \quad (\textit{mid-edge nodes}) \end{cases} \tag{25}$$

Shape functions of an element satisfy the following criterion at all points inside the element:

$$\sum_{n=1}^{N} N_n^{(e)}(x,y,z) = 1. \tag{26}$$

In the next, flux approximation is situated in the sentences of the variational principle for each element as follows:

$$\int_{V_e} (S\phi)\mathrm{d}V = \int_{V_e} (S_e \mathbf{N}^{(e)\mathrm{T}}.\Psi^{(e)})\mathrm{d}V = [\int_{V_e} S_e \mathbf{N}^{(e)\mathrm{T}}\mathrm{d}V].\Psi^{(e)} = I_1^{(e)}.\Psi^{(e)} \tag{27}$$

$$\int_{V_e} (\phi\Sigma_a\phi)\mathrm{d}V = \Psi^{(e)\mathrm{T}}.[\int_{V_e} \mathbf{N}^{(e)}\Sigma_a^{(e)}\mathbf{N}^{(e)\mathrm{T}}\mathrm{d}V].\Psi^{(e)} = \Psi^{(e)\mathrm{T}}.\mathbf{I}_2^{(e)}.\Psi^{(e)} \tag{28}$$

$$\int_{V_e} (\nabla\phi.D\nabla\phi)\mathrm{d}V = \Psi^{(e)\mathrm{T}}.[\int_{V_e} \nabla\mathbf{N}^{(e)}D^{(e)}\nabla\mathbf{N}^{(e)\mathrm{T}}\mathrm{d}V].\Psi^{(e)} = \Psi^{(e)\mathrm{T}}.\mathbf{I}_3^{(e)}.\Psi^{(e)} \tag{29}$$

$$\frac{1}{\alpha^2}\int_{S_b} \phi^2\mathrm{d}S = \Psi^{(e)\mathrm{T}}.[\int_{\partial V_e} \lambda\mathbf{N}^{(e)}.\mathbf{N}^{(e)\mathrm{T}}\mathrm{d}S].\Psi^{(e)} \tag{30}$$

In Eq. (30), λ is a constant that for perfect reflective boundary condition is set to zero and at vacuum boundaries is equivalent to 0.5, according to Eq. (14).

Finally, all elements are assembled to form a monolithic system of linear equations for the overall system:

$$K'[\phi] = \bigcup_{e=1}^{N_p} (2\mathbf{I}_1^{(e)}.\Psi^{(e)} - \Psi^{(e)\mathrm{T}}.(\mathbf{I}_2^{(e)} + \mathbf{I}_3^{(e)} + \mathbf{I}_4^{(e)}).\Psi^{(e)}) = 2\Psi^{\mathrm{T}}.\mathbf{S} - \Psi^{\mathrm{T}}.\mathbf{M}.\Psi \tag{31}$$

where $\bigcup$ is a symbol for the assembly procedure of N_p elements, $\mathbf{S}$ and $\mathbf{M}$ are the global source and coefficient matrices, and Ψ is the global neutron flux vector. Maximizing Eq. (31) through vanishing the first variation of $K'[\phi]$ with respect to Ψ results in the following linear system of equations:

$$\mathbf{M}.\Psi = \mathbf{S}. \tag{32}$$

In case of fission source in the system, we have

$$\mathrm{S} = \frac{1}{k_{eff}}\nu\Sigma_f^{(e)}\phi \tag{33}$$

Here, Eq. (27) is rewritten as:

$$\int_{V_e} (\mathrm{S}\phi)\mathrm{d}V = \frac{1}{k_{eff}}\nu\Sigma_f^{(e)}\int_{V_e} \varphi^2\mathrm{d}V = \Psi^{(e)\mathrm{T}}.[\nu\Sigma_f^{(e)}\int_{V_e} \mathbf{N}^{(e)}.\mathbf{N}^{(e)\mathrm{T}}\mathrm{d}V].\Psi^{(e)} = \Psi^{(e)\mathrm{T}}.\mathbf{I}_f^{(e)}.\Psi^{(e)} \tag{34}$$

Now, we have a system of equations which is an eigenvalue problem solved by the power iteration method. For this case, $\mathbf{S}$ vector is obtained as

$$\mathbf{S} = \mathbf{I}_f.\Psi_0 \tag{35}$$

where Ψ_0 is an initial guess for the flux vector to start the iteration procedure. Eventually, for a multi-group system of equations, the neutron multiplication factor and flux are calculated in each of energy group by using an initial guess for the group flux.

3.2 Adjoint neutron diffusion equation

It should be noted that the adjoint operator would be the transpose of the direct operator (Bell and Glasstone, 1970; Duderstadt and Hamilton, 1976). Therefore, the multigroup adjoint NDE can be stated as

$$-\nabla.(D_g(r)\nabla\phi_g^\dagger(r)) + \Sigma_{r,g}(r)\phi_g^\dagger(r) = \frac{\nu\Sigma_{f,g}(r)}{k_{eff}}\sum_{g'=1}^{G}\chi_{g'}\phi_{g'}^\dagger(r) + \sum_{g'\neq g}\Sigma_{g\to g'}(r)\phi_{g'}^\dagger(r); \quad g = 1,2,...,G \tag{36}$$

where $\phi_g^\dagger$ is the group adjoint function fallaciously (but commonly) referred to as flux. Similarities between Eqs. (36) and (20) reveals that the same algorithm used to solve the forward NDE can also be applied for the adjoint counterpart, with minor changes in the role of some of components, *e.g.* exchange between $\nu\Sigma_{f,g}$ and $\chi_{g'}$ or energy levels in $\Sigma_{g\to g'}(r)$.

4 Numerical examples

Based on the proposed methodology a computer code, GELES, was developed to solve multigroup forward and adjoint NDE for arbitrary shaped 3D systems. To validate the method, two benchmark problems are studied in this section.

4.1 The IAEA-3D benchmark

The IAEA-3D benchmark (Center, 1977) describes a PWR with typical cross sections for the fuel assemblies and partly inserted control rods. The active core height is 340 cm, covered with axial and radial reflectors. The geometry of the IAEA-3D reactor with 15 assemblies across the core diameter is shown in Fig. 4, and material constants are listed in Table 1. The boundary conditions of the reactor core comprise of no incoming current for external boundaries and perfect reflective for the symmetry line boundaries.

Fig. 5 displays a discretized model of the IAEA-3D reactor core using mesh generator. Because of symmetry, only 1/8 of the reactor is needed to be simulated. Results of the calculations using the GELES code is reflected in Table 2. Relative percent error (RPE) in the following tables and figures is defined as

$$RPE = \frac{calculated\ value - reference\ value}{reference\ value} \times 100 \tag{37}$$

Note that the calculated adjoint multiplication factor was the same as its forward counterpart, as anticipated, hence not repeated in a different table. Finally, calculated power distribution is compared with the reference data in Fig. 6.

Figures 7 and 8 show the calculated fast and thermal neutron flux distributions using GELES computer code. It should be noted that the calculated values of the flux are normalized to the unit neutron production rate as follows:

$$\|\phi_g(r)\|_{NPR} = \frac{\phi_g(r)}{NPR} = \frac{\phi_g(r)}{\sum_g^G\sum_e^E\int_{V_e}\nu\Sigma_{f,g}^e\phi_g^e(r)\mathrm{d}V} \cong \frac{\phi_g(r)}{\sum_g^G\sum_e^E(\nu\Sigma_{f,g}^e\mathbf{I}_1^{eT}.\phi_g^e)} \tag{38}$$

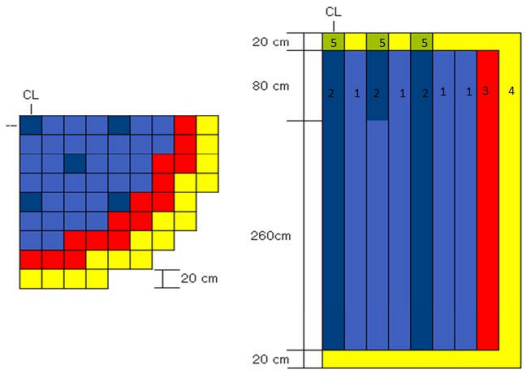

Figure 4: Configuration of the IAEA-3D benchmark problem.

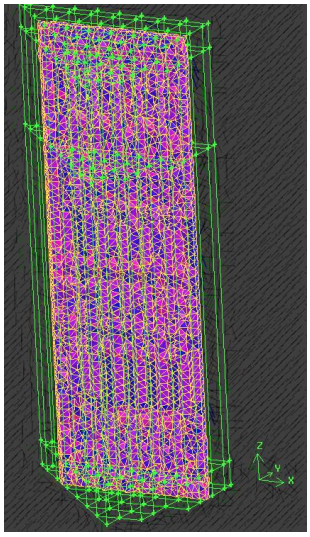

Figure 5: Meshed view of the IAEA-3D reactor core (1/8 symmetry).

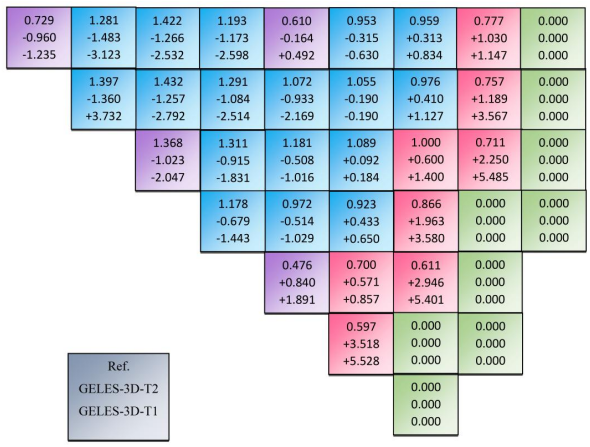

Figure 6: Power distribution in the IAEA-3D reactor core using the GELES computer code.

Table 1: Material cross sections for the IAEA-3D benchmark problem.

Mat. type	g	$D_g(cm)$	Σ_g^r (cm^{-1})	$\Sigma_{1\to g}^s$ (cm^{-1})	$\nu\Sigma_g^f$ (cm^{-1})
1	1	1.500	0.030	0	0
	2	0.400	0.085	0.02	0.135
2	1	1.500	0.030	0	0
	2	0.400	0.130	0.02	0.135
3	1	1.500	0.030	0	0
	2	0.400	0.080	0.02	0.135
4	1	2.000	0.040	0	0
	2	0.300	0.010	0.04	0
5	1	2.000	0.040	0	0
	2	0.300	0.055	0.04	0

Table 2: The calculated neutron multiplication factor for the IAEA-3D benchmark.

Number of elements	App. order	k_{eff}		RPE*	
		GELES-3D	DONJON4	GELES-3D	DONJON4
36,287	Linear	1.03064	1.02884	0.1565	-0.0185
	Quadratic	1.02923	1.02902	0.0194	-0.0010
59,248	Linear	1.03037	1.02892	0.1302	-0.0107
	Quadratic	1.02918	1.02902	0.0146	-0.0010
92,008	Linear	1.02961	1.02897	0.0564	-0.0058
	Quadratic	1.02910	1.02903	0.0068	0.0000

* Relative Percent Error with respect to the reference eigenvalue: k_{eff}=1.02903 (Center, 1977).

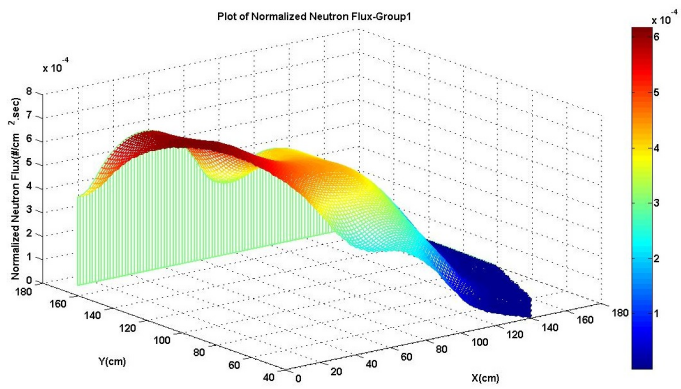

Figure 7: Fast neutron flux distribution in the IAEA-3D reactor core using the GELES computer code.

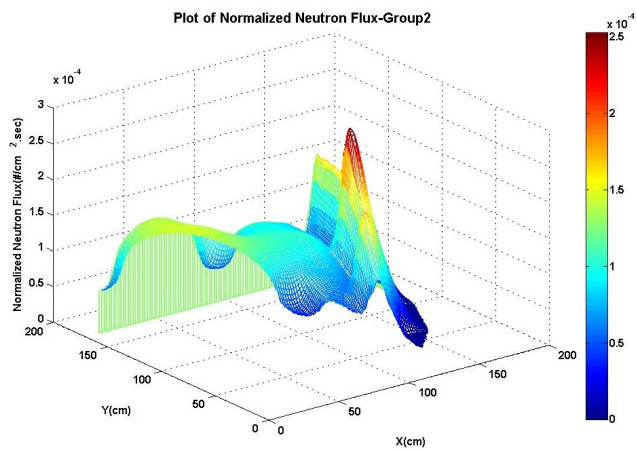

Figure 8: Thermal neutron flux distribution in the IAEA-3D reactor core using the GELES computer code.

4.2 The Schulz PWR benchmark

The 3D Schulz PWR benchmark (Kolev et al., 1999; Schulz, 1996) consists of a VVER-1000 core in the steady state. Hexagonal assemblies are homogeneous in two energy groups and there are seven material compositions including four enrichments, burnable absorber, control rods and reflector. The core height is 355 cm, covered with axial and radial reflectors and the assembly lattice pitch is 24.1 cm. Fig. 9 displays the 30 degrees sector of the core configuration. Also, Table 3 represents the material cross sections for the problem. Results for Schulz-3D reactor are given in Table 4 and Fig. 10 .

Figures 11 and 12 show the calculated fast and thermal normalized neutron flux distributions using GELES computer code. Also, Figs. 13 and 14 display the calculated fast and thermal normalized adjoint flux distributions using GELES computer code. It is worth noting that the calculated adjoint multiplication factor was the same as its forward counterpart.

It should be noted that the calculated neutron multiplication factors by the DONJON4 code (Hébert et al., 2013) given in Tables 2 and 4 was calculated using structural elements and DUAL selective method which uses a mixed-dual finite element discretization. If the geometry is hexagonal, a Thomas-Raviart-Schneider method is used.

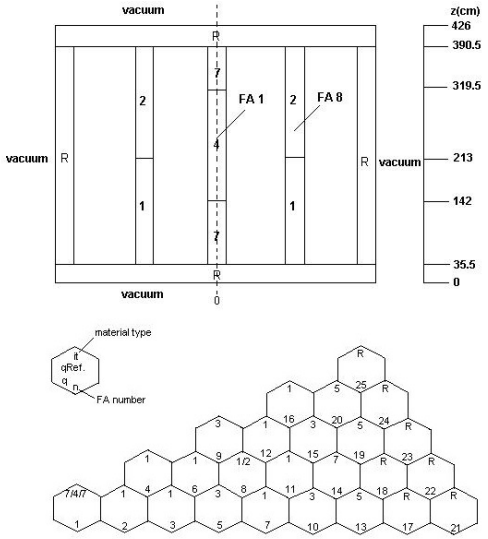

Figure 9: Configuration of Schulz-3D benchmark problem.

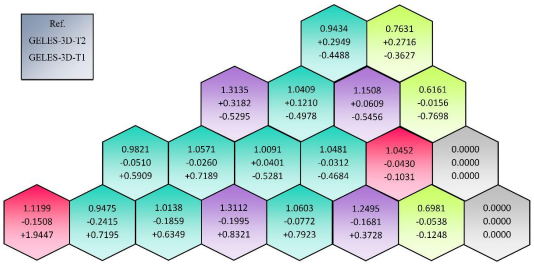

Figure 10: Power distribution in the Schulz-3D reactor core using GELES computer code.

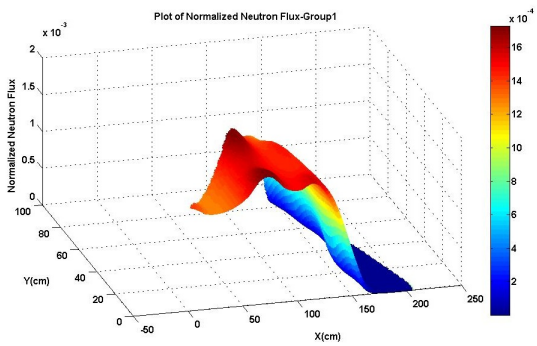

Figure 11: Fast neutron flux distribution in the Schulz-3D reactor core using GELES computer code.

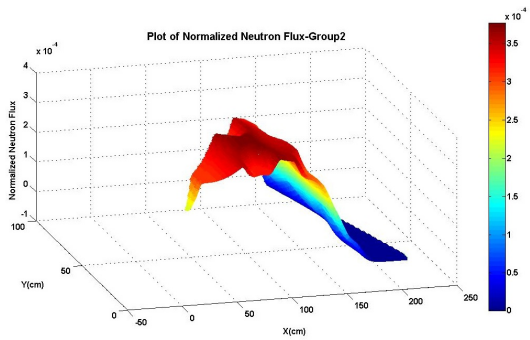

Figure 12: Thermal neutron flux distribution in the Schulz-3D reactor core using GELES computer code.

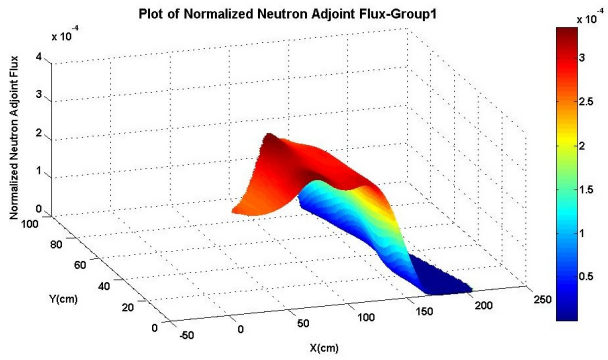

Figure 13: Fast adjoint flux distribution in the Schulz-3D reactor core using GELES computer code.

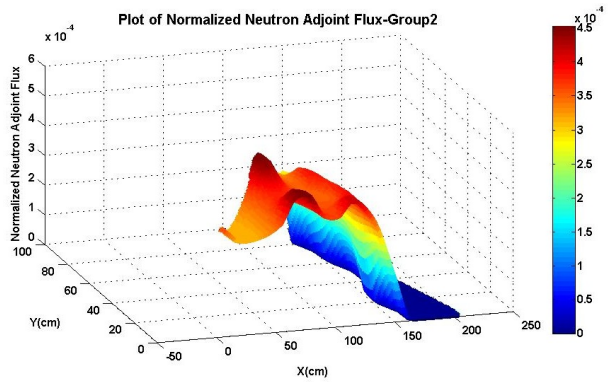

Figure 14: Thermal adjoint flux distribution in the Schulz-3D reactor core using GELES computer code.

5 Discussion

As shown in Tables 2 and 4, differences between the calculated neutron/adjoint multiplication factor and reference value decreases as the number of elements is increased. For the number of 92,008 tetrahedral elements in the IAEA-3D reactor core, the calculated RPE from GELES-3D-T1 (linear), GELES-3D-T2 (quadratic) and DONJON computer codes are 0.0564, 0.0068 and 0.0000, respectively. Also, for the number of 70,950 elements in Schulz-3D reactor core, the calculated RPE from GELES-3D-T1, GELES-3D-T2 and DONJON computer codes are -0.0181, 0.0067 and -0.0029, respectively. Also, the calculated RPEs for power distribution in benchmark problems are in the range of other same reported results (Figs. 6 and 10). Results obtained from the mentioned computer codes have a good agreement with the reference value. The advantage of tetrahedral finite elements over other element types is the suitable accommodation of elements in the boundary layers or regions with high flux gradient. This leads to desired accuracy with low computational cost.

6 Conclusions

In the current study, GELES computer code was developed for multi-group forward/adjoint neutron diffusion calculation based on the generalized least squares finite

Table 3: The material types cross sections for Schulz-3D benchmark problem.

Mat. type	g	$D_g(cm)$	Σ_g^r (cm^{-1})	$\Sigma_{1\to g}^s$ (cm^{-1})	$\nu\Sigma_g^f$(cm^{-1})
1	1	1.37548	0.024135	0	0.0047663
	2	0.38333	0.066002	0.015946	0.083980
2	1	1.40950	0.024769	0	0.004702
	2	0.38756	0.074988	0.014346	0.084128
3	1	1.37067	0.023800	0	0.0058437
	2	0.38028	0.080442	0.015172	0.11468
4	1	1.39447	0.024069	0	0.0061632
	2	0.38549	0.094773	0.013903	0.12598
5	1	1.36938	0.023697	0	0.0063396
	2	0.37877	0.087681	0.014855	0.12998
7	1	1.36966	0.023721	0	0.0062284
	2	0.37911	0.08585	0.014927	0.12612
R	1	1.0	0.040644	0	0
	2	0.33333	0.052785	0.024875	0

Table 4: The calculated neutron multiplication factor for Schulz-3D.

Number of elements	App. order	k_{eff}		RPE*	
		GELES-3D	DONJON4	GELES-3D	DONJON4
34,131	Linear	1.04856	1.04948	-0.0924	-0.0048
	Quadratic	1.04967		0.0133	
62,500	Linear	1.04922	1.04949	-0.0295	-0.0038
	Quadratic	1.04961		0.0076	
70,950	Linear	1.04934	1.04950	-0.0181	-0.0029
	Quadratic	1.04960		0.0067	

* The reference eigenvalue: k_{eff}=1.04953 (Kolev et al., 1999).

elements method. The calculations were performed using tetrahedral finite elements with linear and quadratic approximations for arbitrary shaped 3D geometries. To validate the approach output of GELES were compared against those of DONJON computer code as well as reference data. Acceptable accuracy for the neutron multiplication factor and the power distribution was achieved for all test cases. It is concluded that the GELES code may be used as a reliable and powerful tool for static analysis of 3D multiplying systems.

References

Ackroyd, R. (1986a). A finite element method for diffusion theory embracing nodal and difference methods. *Progress in Nuclear Energy*, 18(1-2):7–20.

Ackroyd, R. T. (1986b). Generalized least squares as a generator of variational principles and weighted residual methods for FEM transport methods. *Progress in Nuclear Energy*, 18(1-2):45–62.

Bell, G. I. and Glasstone, S. (1970). Nuclear Reactor Theory. Technical report, Division of Technical Information, US Atomic Energy Commission.

Cavdar, S. and Ozgener, H. A. (2004). A finite element-boundary element hybrid method for 2-D neutron diffusion calculations. *Annals of Nuclear Energy*, 31(14):1555–1582.

Center, A. C. (1977). ANL Benchmark Book-Report ANL-7416. *Argonne National Laboratory, Argonne, IL.*

Duderstadt, J. J. and Hamilton, L. J. (1976). *Nuclear Reactor Analysis*, volume 1. Wiley New York.

Hébert, A. (2008). A Raviart–Thomas–Schneider solution of the diffusion equation in hexagonal geometry. *Annals of Nuclear Energy*, 35(3):363–376.

Hébert, A., Sekki, D., and Chambon, R. (2013). A User Guide for DONJON Version4. *École Polytechnique de Montréal Montréal QC, Canada, Tech. Rep. IGE-300.*

Kang, C. M. and Hansen, K. F. (1973). Finite element methods for reactor analysis. *Nuclear Science and Engineering*, 51(4):456–495.

Kolev, N., Lenain, R., and Magnaud, C. (1999). AER Benchmark Specification Sheet. *Test ID.: AER–FCM*, 101.

Lamarsh, J. R. (1975). Introduction to Nuclear Engineering.

Lewis, E. E. (1981). Finite element approximation to the even-parity transport equation. In *Advances in Nuclear Science and Technology*, pages 155–225. Springer.

McConnell, A. J. (1951). The hypercircle method of approximation for a system of partial differential equations of the second order. In *Proceedings of the Royal Irish Academy. Section A: Mathematical and Physical Sciences*, volume 54, pages 263–290. JSTOR.

Schulz, G. (1996). Solutions of a 3D VVER-1000 Benchmark. In *Proc. 6-th Symposium of AER on VVER Reactor Physics and Safety, Kirkkonummi, Finland*.

Wang, Y., Bangerth, W., and Ragusa, J. (2009). Three-dimensional h-adaptivity for the multigroup neutron diffusion equations. *Progress in Nuclear Energy*, 51(3):543–555.

Zienkiewicz, O. C. and Taylor, R. L. (2005). *The finite element method for solid and structural mechanics*. Butterworth-heinemann.